**SIZE AND SOLAR INCIDENCE DISTRIBUTION OF SHADOWS ON THE MOON.** Oded Aharonson[1], Paul O. Hayne[2], Norbert Schorghofer[3], [1]Department of Earth and Planetary Sciences, Weizmann Institute of Science, Rehovot, Israel. [2]Jet Propulsion Laboratory, California Institute of Technology, Pasadena, California, USA. [3]Institute for Astronomy, University of Hawaii, Honolulu, Hawaii, USA.

**Overview:** Motivated by the importance of shadows to cold-trapping of volatiles on the Moon and other airless bodies [1], we consider the size distribution of shadows at high incidence angles. We analyzed high-resolution (~1 m/pixel) images from the Lunar Reconnaissance Orbiter (LRO) [2] Narrow-Angle Camera (LROC-NAC) [3] to quantify instantaneous shadowing. A total of 2758 NAC images acquired with solar incidence angles 70 – 89° were analyzed using an automated algorithm to extract shadow patches. These instantaneous shadow fractions were compared to model surfaces composed of varying proportions of craters and rough inter-crater plains. Surface roughness is parameterized by the root-mean-square (RMS) slope of a normal distribution. *Smith* [4] developed analytical formulas for the shadow fraction of random Gaussian surfaces as a function of illumination angle, which compared favorably to the numerical model. We developed analytical expressions for the size of shadows in spherical (bowl-shaped) craters and the ratio of permanent to instantaneous shadow area, and consider the dependence of the shadows on the depth to diameter ratio of the craters [5]. Here we focus on the instantaneous shadows, their distribution of sizes and dependence on incidence angle.

**Results:** Our survey of images demonstrates that small scale (<1 km) shadows contribute non-negligibly to the overall shadow area. Figure 1 shows an example of the analysis performed on an LROC NAC image at incidence angle 87.3°. This image was chosen as it shows an abundance of small shadows, with most of the shadowed area occupied by patches of size <1 km. Other images show different size distributions, some with large patches (> 1 km) dominating the distribution.

Figure 2 shows a histogram of shadow areas for all the images analyzed, as a function of equivalent shadow radius (defined as the radius of a circle with an equivalent area). The distribution is computed in logarithmic size bins and in 1° incidence angle bins. We found the incidence angle dependence of the distributions may be accounted for by a low-order fit; the gray traces thus correspond to different incidence angles in the range explored, with a simple scaling applied. The black trace represents the average of the scaled histograms.

We interpret the size distribution of shadows as follows. At small sizes, below ~3 m, the distribution tails off due finite resolution effect of the images. At large sizes, above ~3 km, the distribution suffers from approaching the finite domain of the images. At the intermediate range the distribution of shadows is reliable and shows an interesting feature. At sizes between ~3 m and ~100 m, the histogram is approximately flat, that is, there is equal shadow area in equal logarithmic size bins. At sizes between ~100 m and ~3 km the histogram is significantly steeper, corresponding to a larger power law exponent. We find a distinct break in slope at ~100 m, indicating a transition of the best-fit power law exponent. We will provide possible interpretations of this feature. Furthermore, we will use the statistical surface model to estimate the areal fraction of permanent shadow over a range of spatial scales.

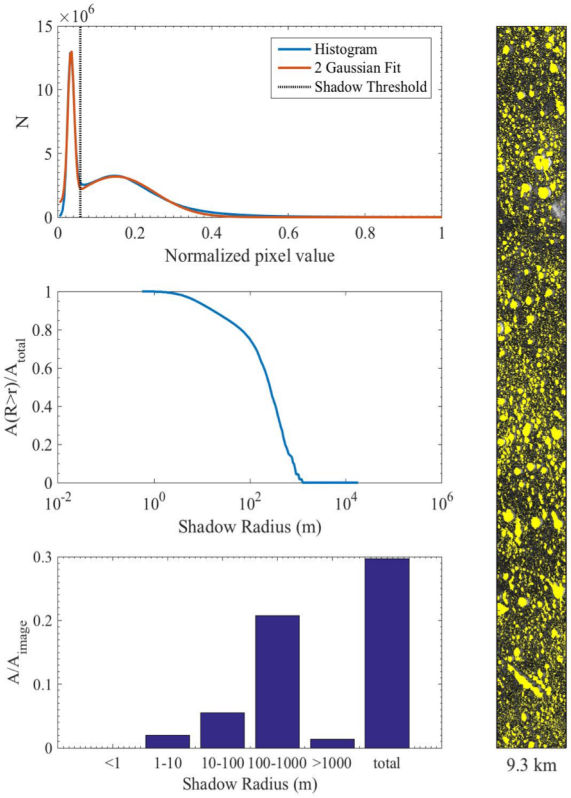


**Figure 1:** An example of the shadow analysis performed on LROC NAC image M102005798LC. The detected shadows are shown on the right panel in yellow. On the left, the panels show histograms of the pixel values used to set a shadow threshold (top), a cumulative distribution of the shadow area as a function of shadow radius, and the differential area distribution in coarse size bins.

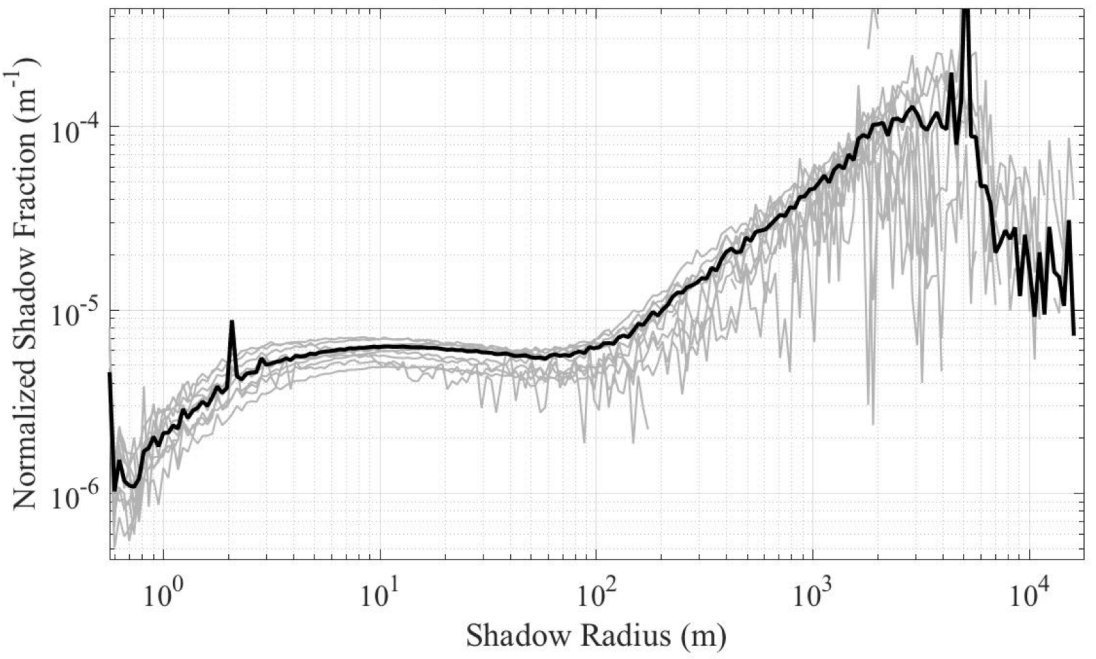


**Figure 2:** A normalized histogram of shadow areas as a function of spatial scale (equivalent shadow radius), computed in logarithmic size bins. The gray traces correspond to different incidence angles in the range explored, with a scaling applied. The black trace represents the average of the scaled histograms.

**References:** [1] Watson, K., et al., *J. Geophys. Res.,* 1961. **66**(9): p. 3033-3045. [2] Keller, J. W., et al., *Icarus*, 2016. **273**: p. 2-24. [3] Robinson, M. S., et al., *Space Sci. Rev.*, 2010. **150**(1): p. 81-124. [4] Smith, B. G., *J. Geophys. Res.*, 1967. **72**(16): p. 4059-4067. [5] Ingersoll, A. P., et al., *Icarus*, 1992. **100**(1): p. 40-47.

**Acknowledgements**: We are thankful for support from the Adolf and Mary Mil Foundation, the Helen Kimmel Center for Planetary Science, the ISF I-CORE program, the Minerva Center grant and from the Lunar Reconnaissance Orbiter project. Part of this work was performed at the Jet Propulsion Laboratory, California Institute of Technology, under contract with the National Aeronautics and Space Administration.